Check for updates

Chemistry-A European Journal



www.chemeurj.org

# **Anions as Lewis Acids in Noncovalent Bonds**

Steve Scheiner\*[a]

The ability of an anion to serve as electron-accepting Lewis acid in a noncovalent bond is assessed via DFT calculations.  $NH_3$  is taken as the common base, and is paired with a host of  $ACI_n^-$  anions, with central atom A=Ca, Sr, Mg, Te, Sb, Hg, Zn, Ag, Ga, Ti, Sn, I, and B. Each anion reacts through its  $\sigma$  or  $\pi$ -hole although the electrostatic potential of this hole is quite

negative in most cases. Despite the contact between this negative hole and the negative region of the approaching nucleophile, the electrostatic component of the interaction energy of each bond is highly favorable, and accounts for more than half of the total attractive energy. The double negative charge of dianions precludes a stable complex with NH<sub>3</sub>.

## Introduction

Since its inception in the early  $20^{th}$  century, the H-bond has developed into the most influential of all noncovalent bonds. It is intimately involved in the structure and function of a full range of biological macromolecules, solvation phenomena, and catalysis, to name just a few. The simplest schematic of a H-bond is denoted by AH..D where a certain amount of electron density is released by the electron donor group D to the proton donor AH. The source of this density is typically a lone electron pair on D, but a  $\pi$ -bond or extended conjugated  $\pi$ -system is a common alternate, as well as a  $\sigma$ -bonding orbital in certain cases. This charge transfer is supplemented by a coulombic attraction between the partial positive charge on the bridging proton and a negative region on D.

Recent years have witnessed the blossoming of the study of a group of interactions that bear a close resemblance to the Hbond, except that the central H is replaced by any of a wide gamut of other atoms, i.e. A-X.[8-26] These noncovalent bonds have the same roots as does the H-bond, and are quite comparable in strength. The principal distinction is that whereas the partial positive charge of H is dispersed over its entirety, the positive region of the analogous bridging atoms is localized in a small region directed along the extension of the A-X covalent bond, an area that has been christened the  $\sigma$ -hole. Thus, even an electronegative atom like CI has a positive  $\sigma$ -hole, that is surrounded by a much more negative region, leaving CI with an overall partial negative charge. It has become common practice to subclassify each sort of  $\sigma$ -hole bond by the group name of the X atom which has replaced the H, as for example halogen, chalcogen, pnicogen bonds, and so forth. These same generic names are generally applied also to bonds where the positive region lies not along a bond axis, but rather above the plane of the molecule, in which case it is designated as a  $\pi$ hole.

A proliferation of ongoing research has documented the importance of these noncovalent bonds to an astonishing array

of chemical processes, from catalysis<sup>[27–31]</sup> to crystal engineering,<sup>[32–39]</sup> from protein binding and structure<sup>[19,40–44]</sup> to enzyme activity<sup>[45,46]</sup> and conformational equilibria<sup>[47–50]</sup> and other biological functions,<sup>[51–57]</sup> as well as ion transport<sup>[26,58–60]</sup> and perovskite semiconductors<sup>[61]</sup> or tunable photoswitches.<sup>[62,63]</sup> The widespread presence and implications of these bonds make it crucial to develop a thorough understanding of their fundamental underpinnings and means of manipulating them.

As one might expect, it has been found that the strength of any given noncovalent bond of this sort is closely related to the intensity of the positive region on the X atom, i.e. the depth of the  $\sigma$  or  $\pi$ -hole. This property is usually quantified as the maximum of the molecular electrostatic potential (MEP) on an isodensity surface surrounding the X center, frequently but not always  $\rho\!=\!0.001$  au. (This density is thought to roughly correspond to the van der Waals radius, encompassing the bulk of the total electron density.) More specifically, the strength of many such noncovalent bonds have been found to be roughly proportional to the value of this maximum,  $V_{\text{max}}$ . (It goes without saying that the magnitude of the negative minimum in the potential of the Lewis base  $V_{\text{min}}$  also plays an important role in the electrostatic interaction.)

From the forgoing description, it would be natural to conclude that imposition of a negative charge on the Lewis acid ought to repel any incoming nucleophile, and preclude any attractive interaction at all. Even if the atom in question contained an electron deficiency in the expected region, the resulting  $\sigma$  or  $\pi\text{-hole}$  in its MEP would likely be negative in sign. Yet, the recent literature is lightly sprinkled with a small number of exceptions to this supposition. That is, several disparate systems contain a noncovalent bond despite an anionic Lewis acid with a negatively charged  $\sigma$  or  $\pi$ -hole. Due to its anionic character, the  $\pi$ -hole lying above the BeCl<sub>3</sub><sup>-</sup> plane is negative, yet it can bind to either NCH or pyridine. [64] The same applies to the  $\sigma$ -hole of  $ZCl_4^-$ , where Z refers to P, As, or Sb, which can engage in a stable pnicogen bond.  $^{[65]}$  On the other hand, the  $\pi$ hole lying above the AeX<sub>5</sub><sup>-</sup> anion (Ae=Kr or Xe) is unable<sup>[66]</sup> to form a noncovalent bond. The situation is further complicated in that there have been a number of  $\mathsf{cases}^{[67,68]}$  where analysis of a specific crystal structure was suggestive of perhaps some level of noncovalent bonding involving a negative  $\pi$ -hole, but it was unclear if this dyad would exist in the absence of the

Department of Chemistry and Biochemistry, Utah State University, Logan, Utah 84322-0300, USA

E-mail: steve.scheiner@usu.edu

<sup>[</sup>a] S. Scheiner

geometric constraints imposed by crystal packing effects that force them together.

There are thus a set of important fundamental questions that remain to be resolved. Is it possible for an anion with a negative  $\sigma$  or  $\pi$ -hole to act as Lewis acid in a noncovalent bond with a neutral nucleophile, and if so under what conditions? Is there a limit on the negative value of this hole beyond which no such bond is possible? Are certain classes of atoms particularly amenable to such a bond, e.g. chalcogen, pnicogen, or transition metals of a given group, or do similar rules apply to all? Is there a fundamental distinction in this regard between  $\sigma$  and  $\pi$ -holes, and how does the shape of the Lewis acid anion play into this scenario. How strong might these bonds be, and how closely is bond strength tied to the quantitative value of the negative hole?

The quantum chemical calculations described here address these questions in a systematic manner. A wide range of anions are considered, each of which contains either a  $\sigma$  or  $\pi$ -hole associated with a central atom. The values of  $V_{\text{max}}$  for these potential Lewis acids span a wide spectrum, from positive to deeply negative. The central atom is drawn from a large pool that comprises alkaline earth atoms, chalcogen, pnicogen, tetrel, triel, halogen, and an assortment of transition state elements. Not only anions, but dianions are considered as well. The shapes of these anions are also highly varied, from planar to pyramidal, bipyramidal, and tetrahedral. Also spanning a range is the number of lone pairs assigned to the central atom, which affects the direction and magnitude of any holes.

# Methods

Quantum chemical calculations were performed via the density functional theory (DFT) approach, within the context of the M06-2X functional<sup>[69]</sup> in conjunction with a polarized triple- $\zeta$  def2-TZVP basis set. This combination has been assessed and tested as highly accurate for interactions of the sort examined here.<sup>[70-77]</sup> The Gaussian  $16^{[78]}$  program was chosen as the

specific means to conduct these computations. Interaction energies were calculated as the difference between the energy of the entire complex, and that of the sum of the two constituent subunits within the geometry of the fully optimized dyad. Interaction energies were corrected for basis set superposition error through the standard Boys-Bernardi counterpoise protocol.<sup>[79]</sup>

Maxima in the Molecular Electrostatic Potential (MEP) were measured on the 0.001 au isodensity surface by the Multiwfn program<sup>[80]</sup> which was also used to elucidate ELF diagrams. Atoms in Molecules (AIM) bond paths and their associated critical points<sup>[81]</sup> were located and their properties evaluated with the aid of AIMAII.<sup>[82]</sup> Total interaction energies were decomposed into their contributing constituents by Symmetry-Adapted Perturbation Theory (SAPT)<sup>[83,84]</sup> at the SAPTO level through the PSI4 program<sup>[85]</sup> in the context of the same def2-TZVP basis set.

## Results

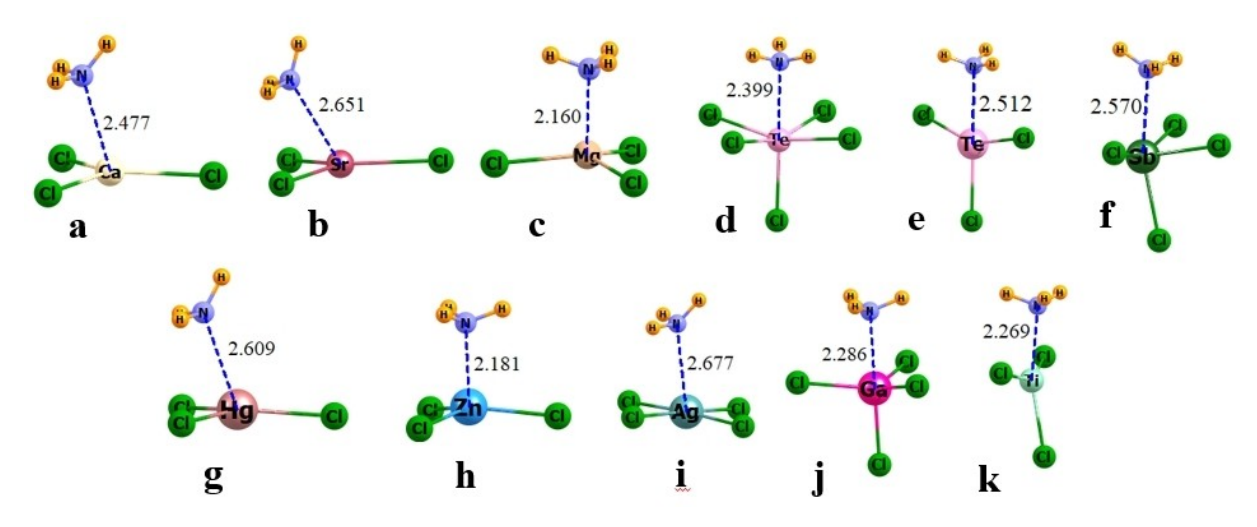
So as to maximize consistency, each of the anionic Lewis acids described below was paired with NH<sub>3</sub> as the common nucleophile. This molecule was chosen for several reasons. In the first place, it is a fairly strong base which ought to provide a solid testing ground for the ability of each Lewis acid to form a noncovalent bond. As an added benefit, with its single lone pair, coupled with its small size, NH<sub>3</sub> will engage in few secondary interactions that might otherwise complicate the analysis of the computed data.

### Structures and Energetics

The optimized geometries of the complexes of NH<sub>3</sub> with the assortment of molecules with which it forms a stable dyad are presented in Figure 1. Table 1 describes some of the salient attributes of each Lewis acid molecule, and most particularly

	Hole	LPs	$V_{max}$	$-E_{int}$	Shape
CaCl <sub>3</sub> <sup>-</sup>	π	0	+ 28.8	19.20	Planar
SrCl <sub>3</sub> <sup>-</sup>	π	0	+24.6	18.28	Planar
MgCl <sub>3</sub> <sup>-</sup>	π	0	-29.2	20.87	planar
TeCl <sub>5</sub>	σ	1	-54.2	18.99	Sq pyr
TeCl <sub>3</sub> <sup>-</sup>	σ π	2	−55.7 −93.5	11.20 X	Planar-T
SbCl <sub>4</sub> <sup>-</sup>	σ	1	-56.9	11.13	trig bipyr
HgCl <sub>3</sub> <sup>-</sup>	π	0	-57.6	9.34	planar
ZnCl <sub>3</sub> <sup>-</sup>	π	0	-58.1	17.39	planar
AgCl <sub>4</sub> <sup>-</sup>	π	0	-67.1	2.96	planar
GaCl <sub>4</sub> <sup>-</sup>	$\Sigma$	0	-84.5	10.31	trig bipyr
TiCl <sub>3</sub> -	П	1(d <sub>z</sub> 2)	-91.1	21.25	planar





 $\textbf{Figure 1.} \ \, \textbf{Optimized geometries of NH}_3 \ \, \textbf{with a)} \ \, \textbf{CaCl}_3^-, \textbf{b)} \ \, \textbf{SrCl}_3^-, \textbf{c)} \ \, \textbf{MgCl}_3^-, \textbf{d)} \ \, \textbf{TeCl}_5^-, \textbf{e)} \ \, \textbf{TeCl}_5^-, \textbf{e)} \ \, \textbf{TeCl}_3^-, \textbf{f)} \ \, \textbf{SnCl}_4^-, \textbf{g)} \ \, \textbf{MgCl}_4^-, \textbf{j)} \ \, \textbf{GaCl}_4^-, \textbf{k)} \ \, \textbf{TiCl}_3^-, \textbf{k)} \ \, \textbf{TiC$ distances in Å.

the properties of the  $\pi$  or  $\sigma$ -hole which attracts the nucleophilic NH<sub>3</sub>. The systems are ordered in Table 1 in diminishing value of V<sub>max</sub>, the maximum of the molecular electrostatic potential (MEP) on the 0.001 au isodensity surface of the optimized monomer. Note especially that while this quantity is positive for the  $CaCl_3^-$  and  $SrCl_3^-$  anions, it quickly turns negative as one proceeds down the list, dropping down to nearly -100 kcal/ mol.

Also reported in Table 1 is the number of lone pairs on each monomer, as evaluated by a depiction of the ELF diagram of each. The number and placement of these lone pairs have an impact on the location of the MEP maxima and the geometry of each dyad. Note that several of these Lewis acid anions have a simple planar shape with a  $\pi$ -hole lying over the central A atom, whether trigonal or square, with no lone pairs to complicate the binding. The lone pair on TeCl<sub>5</sub><sup>-</sup> leads to an overall square pyramidal shape, where the Te lone pair is coincident with the  $\sigma$ -hole lying opposite the apical CI, as illustrated in Figure 2a. The situation in TeCl<sub>3</sub><sup>-</sup> is a bit more complicated, in that the structure of this uncomplexed anion is trigonal bipyramid, with

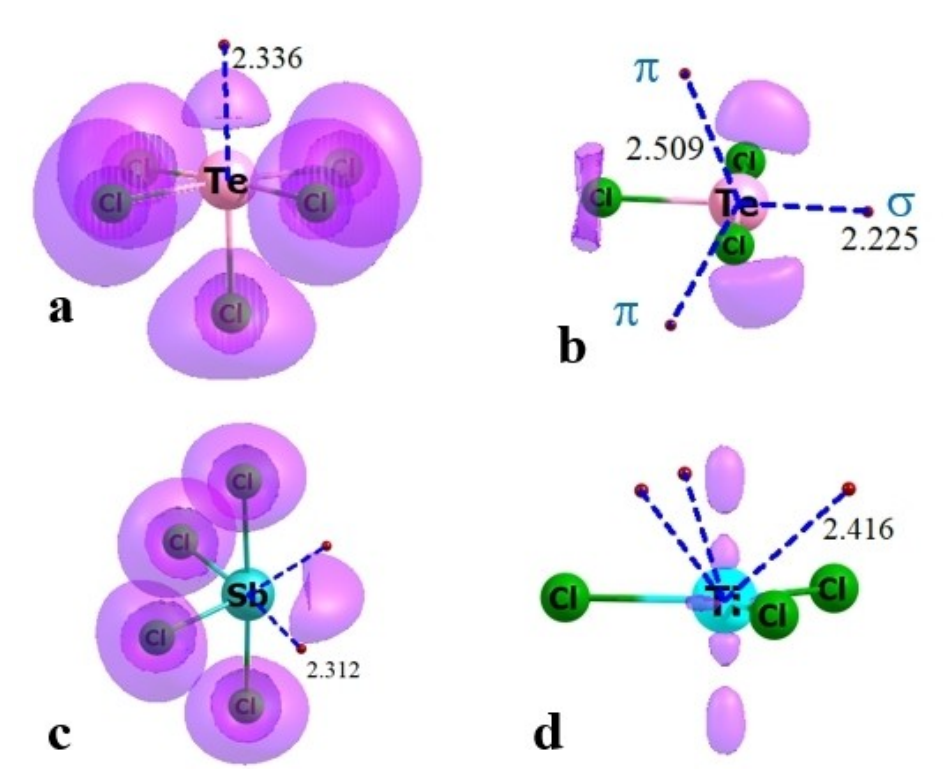


Figure 2. Positioning of MEP maxima (red dots) amidst ELF diagrams of a) TeCl<sub>3</sub>, b) TeCl<sub>3</sub>, c) SbCl<sub>4</sub>, and d) TiCl<sub>3</sub>. Distances of maxima from central atom in Å.

its Te lone pairs occupying two of the equatorial sites. There is one σ-hole directly opposite the remaining equatorial Cl, lying between the two Te Ione pairs, as depicted in Figure 2b. There are also two other maxima in the equatorial plane, both also avoiding the Te Ione pairs. These two are characterized here as  $\pi$ -holes as they lie above and below the molecular plane. As may be seen in Table 1, these  $\pi$ -holes are much more negative than is the  $\sigma$ -hole. SbCl<sub>4</sub><sup>-</sup> takes a similar trigonal bipyramid shape as does TeCl<sub>3</sub><sup>-</sup>, but with only one equatorial lone pair. There are two  $\sigma$ -holes, each lying opposite one of the equatorial CI centers, spaced on either side of the Sb lone pair, as indicated in Figure 2c. The single lone pair of TiCl<sub>3</sub><sup>-</sup> is of d<sub>z</sub>2 type so is equally disposed above and below the molecular plane in Figure 2d. The three  $V_{\text{\scriptsize max}}$  above the plane are spread out to avoid this lone pair, so are each situated roughly above a Cl-Ti-Cl bisector. Given their position above the plane, they are designated here as  $\pi$ -holes, as in the case of TeCl<sub>3</sub><sup>-</sup>.

The interaction energies between NH<sub>3</sub> and each Lewis acid anion, as reported in Table 1, run a wide range between 3 and 21 kcal/mol. There is no obvious correlation between  $E_{int}$  and the depth of the corresponding  $\sigma$  or  $\pi$ -hole. Indeed, the most negative  $V_{max}$  in Table 1 for  $TiCl_3^-$  of -91 kcal/mol is associated with the strongest interaction energy of 21.25 kcal/mol, while values of  $-E_{int}$  only slightly smaller arise for  $CaCl_3^-$  and  $SrCl_3^-$  with their positive  $V_{max}$ . The  $\pi$ -hole location of  $TeCl_3^-$  cannot sustain a bonding interaction with NH<sub>3</sub>, even though its  $V_{max}$  is only slightly more negative than that of  $TiCl_3^-$ .

A secondary issue has to do with irregularities in the geometries of some of the complexes in Figure 1. It might be noted, for instance, that the NH<sub>3</sub> does not lie directly above the Ca or Sr, but is skewed off to one side, where two of its H atoms can form a stabilizing weak NH··Cl interaction. This off-center positioning does not affect the energies much. For example, forcing the N to lie directly above the Sr reduces the interaction energy between SrCl<sub>3</sub><sup>-</sup> and NH<sub>3</sub> by only 1.1 kcal/mol.

Given the negative MEP on the Lewis acid and the lone pair of the NH<sub>3</sub>, one would expect a Coulombic repulsion to be the result. SAPT decomposition of the interaction energies of the various dyads show the opposite to be the case. The electrostatic (ES) components in Table 2 are quite negative and attractive for all complexes. ES varies from a minimum of  $-15\,\rm kcal/mol$  for  $\rm AgCl_4^-$  all the way up to  $-57\,\rm kcal/mol$  for  $\rm TiCl_3^-$ . Indeed, ES is the single largest attractive component in Table 2, accounting for well over half of the total of the three attractive terms. It is worth noting as well that there is little relationship between ES and  $\rm V_{max}$  on the monomer.

There are several reasons that ES takes a negative value. In the first place, it is overly simplistic to look at the total electrostatic term as arising only from the interaction between the  $\sigma/\pi$ -hole and the N lone pair. The H atoms of NH $_3$ , for example, are surrounded by a positive MEP which will be attracted to the anion. Secondly, there is a charge penetration aspect to ES which would make this term more negative. This penetration is accentuated by the fairly short intermolecular distances of the complexes exhibited in Figure 1, all well below 3 Å, and some even approaching 2 Å. Regarding the two other

Table 2. SAPT components of interaction energy of complexes with NH<sub>3</sub>, DISP ES EX IND CaCl<sub>3</sub> -36.6830.69 -6.99-5.53SrCl<sub>3</sub> -29.0923.40 -6.70-5.63MgCl<sub>3</sub> -44.6438.55 -9.04-6.50TeCl<sub>5</sub> -57.2681.81 -34.81-18.07TeCl<sub>3</sub> -37.7753.47 -19.52-12.38SbCl<sub>4</sub> -36.3249.94 -16.49-12.39 HgCl<sub>3</sub> -23.3526.62 -7.15-8.25ZnCl<sub>3</sub> -51.4751.78 -11.20-8.88AgCl<sub>4</sub>--14.9119.14 -3.52-7.14GaCl<sub>4</sub> -54.9870.21 -16.90-13.34TiCl<sub>3</sub> -57.3361.72 -14.23-11.33

attractive components, induction (IND) is second to ES although much smaller in magnitude, followed by dispersion (DISP).

# **Geometrical and Electron Density Considerations**

The short intermolecular distances in some of these complexes brings up the question as to whether the bonding ought to be classified as noncovalent or covalent. The interaction energies are generally below 20 kcal/mol, so might best fit the noncovalent descriptor. An alternative view takes account of the distances between the pertinent atoms. Since each A atom is of different size, the raw R(A-N) distance might be misleading so this distance was normalized by dividing by the sum of the covalent radii of A and N. These normalized distances are labeled as  $R_{\rm cov}$  and are listed in Table 3 for both A-N and for the internal A–Cl covalent bond as a point of comparison.

Not surprisingly,  $R_{cov}$  for A–Cl hovers within 0.05 of unity, consistent with its characterization as a covalent bond. These normalized bondlengths span a wider range for A–N. The three

Table 3. Bond critical point density (au) and ratio of bond length to sum of covalent bond radii in complexes with NH<sub>3</sub>

	$R_{cov}$		ρво	P
	A-N	A–Cl	A-N	A–Cl
CaCl <sub>3</sub>	1.02	0.95	0.0328	0.0392
SrCl <sub>3</sub> <sup>-</sup>	1.04	0.96	0.0285	0.0353
MgCl <sub>3</sub> <sup>-</sup>	1.03	0.97	0.0363	0.0396
TeCl <sub>5</sub>	1.16	1.06	0.0644	0.0769
TeCl <sub>3</sub> <sup>-</sup>	1.21	1.01	0.0470	0.0693
SbCl <sub>4</sub> <sup>-</sup>	1.22	1.04	0.0406	0.0690
HgCl <sub>3</sub> <sup>-</sup>	1.28	1.05	0.0354	0.0742
ZnCl <sub>3</sub> <sup>-</sup>	1.15	1.06	0.0553	0.0636
AgCl <sub>4</sub> <sup>-</sup>	1.35	1.03	0.0269	0.0799
GaCl <sub>4</sub>	1.17	1.01	0.0483	0.0753
TiCl <sub>3</sub> <sup>-</sup>	1.10	0.99	0.0545	0.0722

 $MCl_3^-$  anions in the first three rows, where M refers to the rare earth metals Ca, Sr, and Mg, are all below 1.05, which is consistent with their interaction energies of roughly 20 kcal/mol. But  $R_{cov}$  is larger for the remaining dyads, varying from 1.10 for  $TiCl_3^-$  up to 1.35 for  $AgCl_4^-$ . These quantities bear a relation with the interaction energies in that  $-E_{int}$  is equal to 21 kcal/mol for the former and is below 3 kcal/mol for the latter. In fact, the correlation coefficient between  $R_{cov}$  and  $E_{int}$  is equal to 0.80. One might take an arbitrary cutoff of 1.1 in  $R_{cov}$  as a demarcation between a covalent and noncovalent bond.

Another perspective on bond characterization emerges through AIM analysis of the bonding patterns. The density of the bond critical point is a commonly accepted metric for bond strength and the values of  $\rho_{\text{BCP}}$  for both sorts of bonds are included as the last two columns of Table 3. The A–Cl bonds appear to be of two sorts.  $\rho_{\text{BCP}}$  is roughly 0.04 au for the three MCl<sub>3</sub> $^-$  anions in the first three rows, but is much larger, in the neighborhood of 0.07–0.08 au for the remaining dyads.

Comparison with the parallel quantities for the A–N interactions affords a measure of their relative bond strength. Again starting with the three  $MCl_3^-$  anions,  $\rho_{BCP}$  for A–N is only slightly smaller than the corresponding A–Cl quantity, suggesting both might be considered as covalent bonds. The former is considerably smaller than A–Cl for the remaining systems. In fact, the ratio between the two BCP densities correlates quite well with the interaction energy, with a correlation coefficient of 0.93, as illustrated in Figure 3. That is, the weakest binding is closely associated with smallest A–N/A–Cl ratio.

There are five systems with a ratio that exceed 0.75 to which one might attribute a strong element of covalency. This group encompasses the three aforementioned  $MCl_3^-$  anions, all with ratios exceeding 0.8, complemented by  $TeCl_5^-$  and  $ZnCl_3^-$ , with a similar ratio; this quantity is slightly smaller at 0.75 for  $TiCl_3^-$ .

#### **Internal Perturbations**

Another measure by which to gauge the covalency of a new interaction is its influence on the geometry of the Lewis acid molecule. Taking the MCl<sub>3</sub><sup>-</sup> units in Figure 1a–c as an example, were the NH<sub>3</sub> to be replaced by a Cl<sup>-</sup>, the planar MCl<sub>3</sub> would be replaced by a tetrahedral MCl<sub>4</sub> shape, albeit with different M–Cl bondlengths. In contrast, Figure 1a–c show that the MCl<sub>3</sub> largely retains its planarity when associated with NH<sub>3</sub> acquiring only a small measure of pyramidal character. This same maintenance of the basic monomer shape is true of all the dyads in Figure 1 which would argue for their characterization as noncovalent bonds.

On the other hand, there are of course some perturbations that are part and parcel of the formation of the new bond, whether noncovalent or covalent. The introduction of a small degree of nonplanarity into the aforementioned MCl<sub>3</sub><sup>-</sup> units is one example. Another is the opening up of the umbrella angle within tetrahedral GaCl<sub>4</sub><sup>-</sup> to permit the approach of the fifth ligand in Figure 1j.

Some of the primary effects of the introduction of the  $NH_3$  ligand are changes in the internal A–Cl bond lengths. These changes are reported in Table 4 along with the related perturbation of the symmetric stretching frequency. (In cases where the asymmetry of the system yields inequivalent Cl atoms, it is the change in their average bond length which is reported.) Inspection of the data in Table 4 reveals a significant A–Cl bond stretch of at least 0.020 Å and as high as 0.066 Å in the case of  $TiCl_3$ . Associated with this weakening of the internal bonds is a red shift of the symmetric A–Cl stretching frequency. The magnitude of this reduction in v is variable, spanning a range between 5 and 43 cm $^{-1}$ .

These changes can be placed in context when compared to the effect of adding a fourth CI to CaCl<sub>3</sub><sup>-</sup> as a clearly covalent

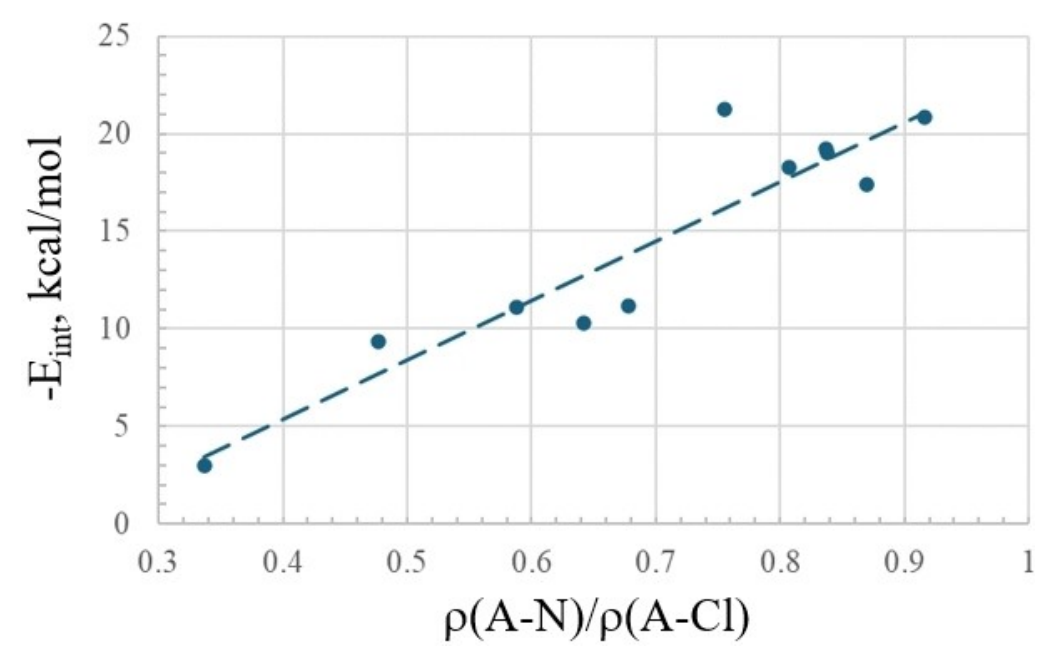


Figure 3. Relationship between interaction energy and ratio of BCP densities.

Chemistry Europe

European Chemical Societies Publishing

oond length and symmetric stretching

Table 4. Changes in internal bond length and symmetric stretching frequency resulting from addition of NH3.  $\Delta r(A-CI)$ , Å  $\Delta v$ , cm<sup>-1</sup> CaCl<sub>3</sub> 0.0397 -12.6SrCl<sub>3</sub>-0.0403 -16.12MgCl<sub>3</sub> 0.0501 -14.2TeCl<sub>5</sub> 0.0736 -17.0TeCl<sub>3</sub>  $-5.5^{[a]}$ 0.0450  $-10.3^{[a]}$ SbCl<sub>4</sub> 0.0543 HgCl<sub>3</sub> 0.0395 -7.0ZnCl<sub>3</sub> 0.0549 -29.8AgCl<sub>4</sub> 0.0198 -10.8GaCl<sub>4</sub> 0.0557 -18.0TiCl<sub>3</sub> 0.0657 -42.6[a] asymmetric stretch.

bond. This addition elongates the Ca–Cl bonds by 0.102 Å, 2.6 times more than does NH<sub>3</sub>. Likewise, there is a nearly threefold reduction in the stretching frequency. This dramatic comparison

argues for the relative weakness of the noncovalent Ca-N versus the covalent Ca-Cl bond.

#### **Restricted Minima**

All of the foregoing dyads represent true minima, with no imaginary harmonic frequencies. When NH<sub>3</sub> was added to several other anions, it tended to rotate around so that it is the positive H atom regions that approach the anion, thereby precluding the occurrence of any sort of A-N bonding. One can prevent this rotation by restricting the A atom of the Lewis base anion to lie along the C<sub>3</sub> rotation axis of NH<sub>3</sub> during the optimization. The resulting structures displayed in Figure 4 are therefore not true minima, but can be analyzed nonetheless for possible noncovalent bonding.

One aspect of the anions listed in Table 5 is the highly negative sign of  $V_{max}$ ,  $-70\,kcal/mol$  or even smaller. It is emphasized that even though coaxed to form dyads by the geometry restriction, the complexes are held together only very tenuously. Interaction energies are less than 3 kcal/mol for the first two rows of Table 5, and turn positive for the others. In fact, even with this geometrical restriction,  $ICl_2^-$  cannot be induced to engage with  $NH_3$  at all, as the two molecules simply

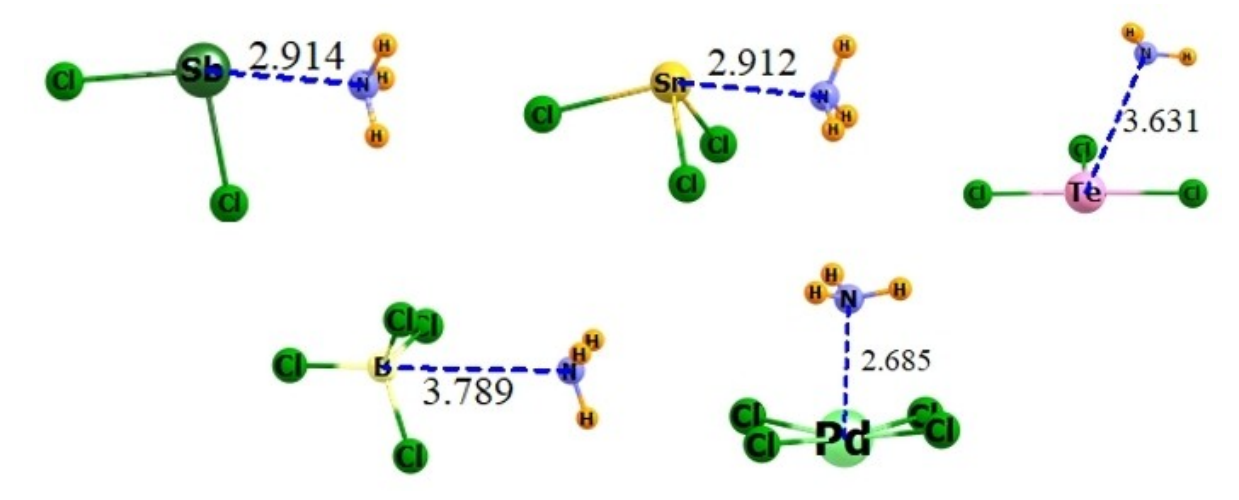


Figure 4. Optimized geometries of complexes with central A atom restricted to C<sub>3</sub> symmetry axis of NH<sub>3</sub>; distances in Å.

<b>Table 5.</b> Characteristics of Lewis acid anions and their complex with NH <sub>3</sub> , with geometry restriction. V <sub>max</sub> and E <sub>int</sub> in kcal/mol.						
	Hole	LPs	$V_{\text{max}}$	$-E_{int}$	Shape	
SbCl <sub>2</sub> <sup>-</sup>	σ	2	-69.7	1.46	Planar	
SnCl <sub>3</sub> <sup>-</sup>	σ	0	-70.4	2.30	Trig pyr	
TeCl <sub>3</sub>	$\pi$	1	-93.6	(-3.02)	Planar T	
ICI <sub>2</sub>	$\pi$	3	-95.9	a	a	
BCl <sub>4</sub> <sup>-</sup>	σ	0	-108.4	(-4.87)	tetrahedral	
$NO_3^-$	$\pi$	0	-112.1	(-5.81)	Trigonal planar	
$PdCl_4^{-2}$	$\pi$	0	-177.7	(-4.42)	Square planar	
$WO_4^-$	σ	0	-205.9	b	tetrahedral	
[a] no dyad, molecules separate. [b] NH <sub>3</sub> inverts.						

repel one another. On the other hand, even with its double negative charge, the  $PdCl_4^{-2}$  anion will interact with  $NH_3$ , even though the total interaction energy is positive. Another dianion  $WO_4^{-2}$ , on the other hand, has such a strong pull on the  $NH_3$  protons that the latter inverts, retaining its  $C_{3v}$  symmetry, so as to form strong NH-O H-bonds.

Considering the totality of the results in Tables 1 and 5, the value of  $V_{max}$  on the central A atom offers some rough guidance as to whether a complex with NH $_3$  might be expected. A negative  $\sigma$  or  $\pi$ -hole with a magnitude of less than about 70 kcal/mol seems capable of forming a stable complex. Any prediction for more negative  $V_{max}$  is cloudier. Despite values of -84.5 and -91.1 kcal/mol, respectively, both  $GaCl_4^-$  and  $TiCl_3^-$  form a stable interaction with NH $_3$  with a substantial interaction energy. The anions in Table 5 require a geometrical restriction to do so, even though two of them have a  $\sigma$ -hole of only -70 kcal/mol.

# Discussion

The values of  $V_{max}$  above were evaluated at an arbitrary distance from each central A atom, namely the point where the total electron density is equal to 0.001 au, as is fairly standard in studies of this sort. Given the favorable electrostatic interaction with the  $NH_3$  nucleophile, as well as the fairly strong binding in these dyads, there is some question as to whether the MEP at this particular point might be deceptive, and would perhaps be positive, or at least very different, if evaluated at some other

point, perhaps closer or more distant from the A center. Such a positive potential would be more conducive to an electrostatic attraction.

Consequently, the MEP was evaluated over a full range of distance d from the central A atom, along a vector perpendicular to the molecular plane of three different anions. As displayed in Figure 5, this potential is fairly stable for distances longer than about 2.4 Å. The MEP is clearly negative for all distances longer than 1.6 Å, much shorter than the A··N intermolecular contact distances in the dyads with NH<sub>3</sub>. It is concluded therefore that the  $\pi\text{-holes}$  in these anions are undoubtedly negative in sign, and their quantitative depth is fairly insensitive to small variations in d.

The results have shown that anions are perfectly capable of acting as Lewis acids in a host of different sorts of noncovalent interactions, including chalcogen, pnicogen, triel, regium, and spodium bonds, among others. The central atoms contain a  $\sigma$  or  $\pi$ -hole, defined as a maximum on an isodensity surface, but this maximum is of negative sign in most cases. These holes can be of both  $\sigma$  or  $\pi$  type, and there are a variety of Lewis acid molecular shapes that lead to these bonding interactions. Despite the sign of the hole, and the negative charge of the anion as a whole, the electrostatic component of its interaction with the negative region of a nucleophile is substantially negative, i.e. attractive. And it is this electrostatic component which accounts for a major share of the total attractive energy.

The magnitude of the  $\sigma$  or  $\pi$ -hole is not a faithful indicator of the ultimate strength of the bond with the nucleophile. Indeed, some of the most negative values of  $V_{max}$  are associated

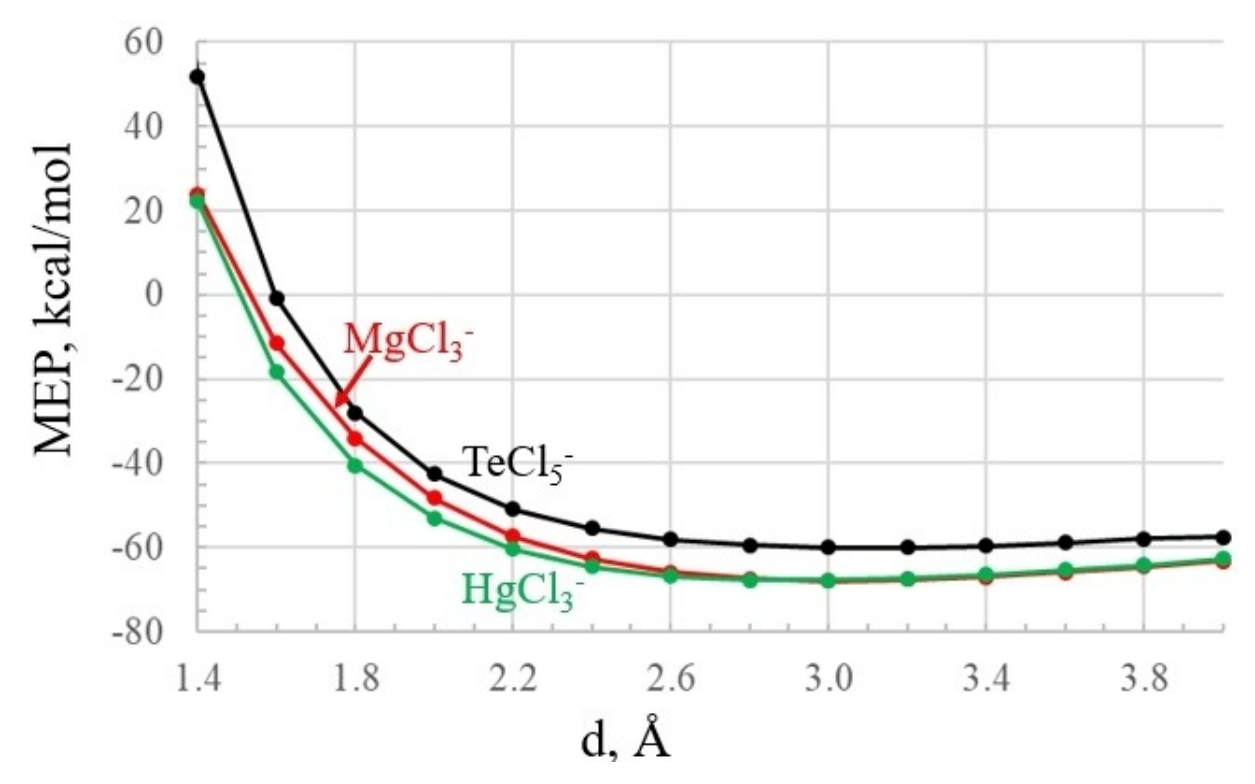


Figure 5. Variation of molecular electrostatic potential with distance d from central A atom, along a vector perpendicular to the molecular plane of indicated anion.

with bond strengths of 20 kcal/mol or so. Moreover, these same highly negative MEPs can result in surprisingly large electrostatic components to the interaction with a nucleophile. Likewise, there are an assortment of anions that are unable to form a noncovalent bond, even with only a modest  $V_{\text{max}}$ . As a very general rule, systems with this quantity more negative than about -70 kcal/mol are reluctant to engage in a bonding interaction with a neutral nucleophile, although two exceptions to this threshold were observed here. Dianions may also contain a  $\sigma$  or  $\pi$ -hole, but with their very negative  $V_{\text{max}}$  in the neighborhood of -200 kcal/mol, are unable to form a viable noncovalent bond.

Some of these bonds have characteristics which make it difficult to unambiguously label them as either noncovalent or covalent. On one hand, the interaction energies are only 20 kcal/mol or less, below what might normally be considered covalent. The modifications in the geometry and spectra of the anion caused by complexation with a nucleophile are small enough that they also lie in the noncovalent domain. The issue becomes cloudier when considering the length and AIM features of the intermolecular bond. Within these contexts, some of these bonds seem to cross over the border into covalency, or at least something close to it.

Some earlier calculations<sup>[64]</sup> had considered various MCl<sub>3</sub>anions where M refers to any of the rare earth metals and their ability to interact through their  $\pi$ -hole with a neutral pyridine N base. The results with a different computational protocol, namely MP2 and CCSD(T) with an aug-cc-pVDZ basis, are consistent with the data in the first rows of Table 1 for NH<sub>3</sub> as base. Moreover, the inclusion of electron correlation with the more accurate CCSD(T) yielded only small changes in the interaction energies. These calculations also verified the large attractive electrostatic components. Likewise, both pyridine and NCH form stable complexes with ZCl<sub>4</sub> where Z represents a pnicogen atom, [65] again with a large ES component. NH3 was shown previously to form a very stable triel bond with TrCl<sub>4</sub>- for Tr atoms larger than Be. [86] The interaction energy of GaCl<sub>4</sub>closely matched the results here with a different computational protocol. As in the other types of bonding, CCSD(T) did not change the MP2 results very much, and again the electrostatic term is quite attractive, accounting for more than 60% of the total attractive components. It was interesting to note<sup>[66]</sup> that neither an anion nor a neutral NCH molecule could engage with a planar AeX<sub>5</sub><sup>-</sup> anion, where Ae refers to a noble gas atom Kr or Xe, even though  $V_{max}$  of the  $\pi$ -hole is between -50 and −70 kcal/mol.

On a related issue, very recent calculations<sup>[87]</sup> have shown that a CI atom located on an anion can engage in a halogen bond. However, this was quite a special case, differing from the situations described here. First, the  $\sigma$ -hole on the CI was positive in sign unlike the negative  $V_{\text{max}}$  of most of the anions considered here. Secondly, and perhaps more important, this bond required the partner of the anion to be a fully charged cation, which would add a great deal of ion pair stability.

Daolio et al have analyzed interactions of the  $\pi$ -hole lying above the Au center of square planar  $\text{AuCl}_4^{-[68]}$  with neutral electron donors. This system is similar to those discussed above

in the sense of a negative  $\pi$ -hole, of magnitude -78 kcal/mol. The authors found evidence of a bonding interaction, but the geometries examined were restricted to what is enforced by crystal packing forces, so there was no attempt to find whether the structures are in fact minima. The results were further complicated in that the binding energy of any Au-O contact was contaminated by several secondary bonds. Given the small interaction energy of the similar AgCl<sub>4</sub><sup>-</sup> anion with NH<sub>3</sub> of 3 kcal/mol found here, it is likely that the interaction would be similarly weak for AuCl<sub>4</sub><sup>-</sup>, especially in light of the even more negative V<sub>max</sub> for the latter anion.

The NO<sub>3</sub><sup>-</sup> anion is another case that highlights some of the issues described here. A recent survey of the CSD showed the  $\pi$ -hole above the N of this anion<sup>[67]</sup> can approach closely to various electron donors, although its  $V_{max}$  is -112 kcal/mol. AIM analysis of several selected structures suggested a binding interaction, but interaction energies were not computed. Also, geometries were taken from crystal structures so it is unclear whether any dimers of this type are true minima or are truly stable to dissociation. Calculations of this anion with the M06-2X/def2TZVP level here verify this  $\pi$ -hole to be -112.1 kcal/mol. According to the calculations described above such a large V<sub>max</sub> would not be conducive to formation of a noncovalent bond. Indeed, an optimization of the dyad between NO<sub>3</sub><sup>-</sup> and NH<sub>3</sub> leads away from a N··N bond and toward a NH··O H-bond instead. In fact, as listed in Table 5, if the N of NO<sub>3</sub><sup>-</sup> is forced to lie along the NH<sub>3</sub> C<sub>3</sub> rotation axis, the interaction is not attractive at all, with an interaction energy of +5.81 kcal/mol. So the structures observed in the CSD with an apparent pnicogen bond to NO<sub>3</sub><sup>-</sup> should probably be attributed to crystal packing forces that hold the two subunits in this orientation. In fact, this contention is verified by calculations of the three protein systems which were the focus of the earlier work. [67] When the groups involved in the EVIKEA, UROHOZ, and BIDHAX model systems are released from the constraints forcing them to hold the positions they occupy within the crystal, they move about in such a way as to delete the pnicogen bond to the N of the NO<sub>3</sub><sup>-</sup> unit.

Another case of the potential of an anion to serve as a Lewis acid arises in the context of a crystal structure where a CI occupies a position on a benzene ring para to a  $SO_3^-$  substituent. Because of its somewhat distant location from the source of negative charge, the  $\sigma$ -hole on this CI atom is slightly positive (+7 kcal/mol) and is thus able to interact in an attractive manner with a N atom, along with a number of other contacts that hold the two subunits together.

A rapidly growing literature is emerging regarding the nature of the interactions between ions of like charge in the context of hydrogen and other noncovalent bonds. [88–113] These systems are different than those discussed above in that the Lewis base is an anion, rather than a neutral NH<sub>3</sub> that is oriented to present its most negative MEP toward the anionic acid. The overall general rule is that pairs of anions are generally repulsive although they can form a metastable dimer, higher in energy than the pair of separated monomers. On the other hand, when placed in their relative positions as in the crystal,

Europe

Chemistry European Chemical Societies Publishing

there are indications of an attractive force that emerge from analysis of the wavefunction.

But there are features of these anion-anion complexes that are of relevance nonetheless. For example, Martín-Fernández et al have emphasized<sup>[114]</sup> that the use of the term "anti-electrostatic" is misleading since these complexes are stabilized by electrostatic forces, echoing a similar sentiment by others.  $^{\left[105,115,116\right]}$  Indeed, the electrostatic component is typically stabilizing even with the two subunits having the same charge. [102,105,109,116-119] There are indications [109] that this component can be repulsive at long range, but then turns attractive for closer approach due in large part to charge penetration. There is the added factor that what is normally considered under the rubric of polarization can in some sense fall under the more general categorization as another manifestation of Coulombic forces. [120] As a final note, there is a significant body of literature that suggests caution be exercised in the application of AIM to establish the presence of bonding interactions between atoms.  $^{\tiny{[120-126]}}$ 

## Conclusions

Despite their overall negative charge, a number of different sorts of anions can serve as electron-accepting Lewis acid with a neutral base within the context of a host of noncovalent bonds. These bonds occur over a wide range of strength, varying from 3 up to more than 21 kcal/mol. The bonding occurs through the intermediacy of a  $\sigma$  or  $\pi$ -hole on the central atom, even though the potential at this hole is clearly negative, and substantially so. Noncovalent bonds are the norm for V<sub>max</sub> less negative than  $-70\,\mathrm{kcal/mol}$ , but can occur for values as large as -90 kcal/mol in certain cases. Even with highly negative MEP on the Lewis acid, the electrostatic component of the interaction energy with a nucleophile is quite attractive, even exceeding 50 kcal/mol. Such bonding is ruled out for dianions.

# **Acknowledgements**

This material is based upon work supported by the National Science Foundation under Grant No. 1954310.

# Conflict of Interests

The author declares no conflict of interest.

# **Data Availability Statement**

The data that support the findings of this study are available from the corresponding author upon reasonable request.

**Keywords:** Sigma-hole • pi-hole • Electrostatic potential • SAPT

- [1] P. Schuster, G. Zundel, C. Sandorfy, The Hydrogen Bond. Recent Developments in Theory and Experiments, North-Holland Publishing Co., Amsterdam 1976.
- S. N. Vinogradov, R. H. Linnell, Hydrogen Bonding, Van Nostrand-Reinhold, New York, 1971.
- [3] E. A. Hillenbrand, S. Scheiner, J. Am. Chem. Soc. 1984, 106, 6266-6273.
- [4] S. M. Cybulski, S. Scheiner, J. Am. Chem. Soc. 1989, 111, 23-31.
- [5] S. Scheiner, Hydrogen Bonding: A Theoretical Perspective, Oxford University Press, New York 1997.
- [6] G. R. Desiraju, T. Steiner, The Weak Hydrogen Bond in Structural Chemistry and Biology, Oxford, New York 1999.
- G. Gilli, P. Gilli, The Nature of the Hydrogen Bond, Oxford University Press, Oxford, UK 2009.
- [8] P. Politzer, J. S. Murray, T. Clark, Phys. Chem. Chem. Phys. 2013, 15, 11178-11189.
- [9] L. M. Azofra, S. Scheiner, J. Chem. Phys. 2015, 142, 034307.
- A. C. Legon, D. G. Lister, J. H. Holloway, D. Mani, E. Arunan, Molecules 2019, 24, 4257.
- [11] G. Sánchez-Sanz, C. Trujillo, I. Alkorta, J. Elguero, ChemPhysChem 2020, 21, 2557-2563.
- [12] S. J. Grabowski, Molecules 2020, 25, 2703.
- [13] I. Iribarren, G. Sánchez-Sanz, I. Alkorta, J. Elguero, C. Trujillo, J. Phys. Chem. A 2021, 125, 4741-4749.
- [14] L. de Azevedo Santos, T. A. Hamlin, T. C. Ramalho, F. M. Bickelhaupt, Phys. Chem. Chem. Phys. 2021, 23, 13842-13852.
- [15] R. D. Parra, S. J. Grabowski, Int. J. Mol. Sci. 2022, 23, 11289.
- [16] S. P. Gnanasekar, E. Arunan, J. Mol. Spectrosc. 2022, 388, 111671.
- [17] R. D. Parra, Science 2022, 4, 9.
- [18] S. A. C. McDowell, N. Liu, Q. Li, Mol. Phys. 2022, 120, e2111374.
- [19] H. S. Biswal, A. K. Sahu, B. Galmés, A. Frontera, D. Chopra, ChemBio-Chem 2022, 23, e202100498.
- [20] K. Konidaris, A. Daolio, A. Pizzi, P. Scilabra, G. Terraneo, S. Quici, J. S. Murray, P. Politzer, G. Resnati, Cryst. Growth Des. 2022, 22, 4987-4995.
- S. J. Grabowski, Phys. Chem. Chem. Phys. 2023, 25, 9636–9647.
- [22] Z. Niu, S. A. C. McDowell, Q. Li, Molecules 2023, 28, 7087.
- [23] M. D. L. N. Piña, A. K. Sahu, A. Frontera, H. S. Biswal, A. Bauzá, Phys. Chem. Chem. Phys. 2023, 25, 12409-12419.
- D. Grödler, S. Burguera, A. Frontera, E. Strub, Chem. Eur. J. 2024, 30, e202400100.
- [25] B. Eftekhari-Sis, I. García-Santos, A. Castiñeiras, G. Mahmoudi, E. Zangrando, A. Frontera, D. A. Safin, CrystEngComm 2024, 26, 1637-
- [26] R. D. Parra, Inorganics 2024, 12, 16.
- X. He, X. Wang, Y.-L. S. Tse, Z. Ke, Y.-Y. Yeung, ACS Catal. 2021, 11, 12632-12642.
- [28] A. A. Sysoeva, A. S. Novikov, M. V. Il'in, V. V. Suslonov, D. S. Bolotin, Org. Biomol. Chem. 2021, 19, 7611-7620.
- [29] A. Boelke, T. J. Kuczmera, E. Lork, B. J. Nachtsheim, Chem. Eur. J. 2021, 27, 13128-13134.
- [30] N. Momiyama, A. Izumiseki, N. Ohtsuka, T. Suzuki, ChemPlusChem **2021**, 86, 913-919.
- [31] Y. Cao, Z. Zhang, W. Lai, T. Yu, Y. Ma, Y. Liu, B. Wang, Cryst. Growth Des. **2022**, 22, 5390-5398.
- [32] V. Nemec, K. Lisac, N. Bedeković, L. Fotović, V. Stilinović, D. Cinčić, CrystEngComm 2021, 23, 3063-3083.
- [33] E. R. T. Tiekink, Coord. Chem. Rev. 2022, 457, 214397.
- [34] P. E. Swathi Krishna, H. C. Babu, N. G. Nair, M. Hariharan, Chem. Asian J. 2023, 18, e202201248.
- [35] R. M. Gomila, E. R. T. Tiekink, A. Frontera, Inorganics 2023, 11, 468.
- [36] J. Vainauskas, T. H. Borchers, M. Arhangelskis, L. J. McCormick McPherson, T.S. Spilfogel, E. Hamzehpoor, F. Topić, S.J. Coles, D.F. Perepichka, C. J. Barrett, T. Friščić, Chem. Sci. 2023, 14, 13031–13041.
- [37] R. M. Gomila, A. Frontera, E. R. T. Tiekink, CrystEngComm 2023, 25, 5262-5285.
- [38] R. M. Gomila, A. Frontera, E. R. T. Tiekink, CrystEngComm 2024, 26, 2784-2795.
- [39] Z. Wang, Z. Cao, A. Hao, P. Xing, Chem. Sci. 2024, 15, 6924–6933.
- [40] V. A. Adhav, K. Saikrishnan, ACS Omega 2023, 8, 22268–22284.
- [41] K. Baruah, D. Kalita, B. Sahariah, J. Kishore Rai Deka, P. Vishnoi, B. Kanta Sarma, Chem. Eur. J. 2023, 29, e202300178.
- [42] J. Li, L. Zhou, Z. Han, L. Wu, J. Zhang, W. Zhu, Z. Xu, J. Med. Chem. **2024**, *67*, 4782-4792.
- [43] V. A. Aliyeva, A. V. Gurbanov, M. F. C. Guedes da Silva, R. M. Gomila, A. Frontera, K. T. Mahmudov, A. J. L. Pombeiro, Cryst. Growth Des. 2024, *24*, 781–791.

Chemistry Europe

European Chemical Societies Publishing

- [44] O. Carugo, Proteins 2023, 91, 395-399.
- [45] E. Y. Tupikina, Org. Biomol. Chem. 2022, 20, 5551-5557.
- [46] R. M. Gomila, A. Frontera, Chem. Asian J. 2024, 19, e202400081.
- [47] S. Mehrparvar, Z. N. Scheller, C. Wölper, G. Haberhauer, J. Am. Chem. Soc. 2021, 143, 19856-19864.
- [48] H. Chen, X. Tang, H. Ye, X. Wang, H. Zheng, Y. Hai, X. Cao, L. You, Org. Lett. 2021, 23, 231-235.
- [49] S. Jia, H. Ye, L. You, Org. Chem. Front. 2022, 9, 3966–3975.
- [50] P. Weng, X. Yan, J. Cao, Z. Li, Y.-B. Jiang, Chem. Commun. 2022, 58, 6461-6464.
- [51] A. Kolarič, T. Germe, M. Hrast, C. E. M. Stevenson, D. M. Lawson, N. P. Burton, J. Vörös, A. Maxwell, N. Minovski, M. Anderluh, Nat. Comm. 2021, 12, 150.
- [52] O. I. Carugo, J. Biomol. Struct. Dyn. 2023, 41, 9576-9582.
- [53] K. Mu, Z. Zhu, A. Abula, C. Peng, W. Zhu, Z. Xu, J. Med. Chem. 2022, 65, 4424-4435.
- [54] M. D. L. N. Piña, A. Bauzá, Int. J. Mol. Sci. 2023, 24, 13035.
- [55] O. Carugo, K. Djinović-Carugo, Front. Mol. Biosci. 2023, 10, 1155629.
- [56] R. M. Gomila, A. Frontera, A. Bauzá, Int. J. Mol. Sci. 2023, 24, 5530.
- [57] G. A. Andolpho, T. C. Ramalho, J. Comput. Chem. 2024, 45, 1303-1315.
- [58] T. Zhao, V. M. Lynch, J. L. Sessler, Org. Biomol. Chem. 2022, 20, 980-983.
- [59] H. Kuhn, A. Docker, P. D. Beer, Chem. Eur. J. 2022, 28, e202201838.
- [60] A. J. Taylor, A. Docker, P. D. Beer, Chem. Asian J. 2023, 18, e202201170.
- [61] P. R. Varadwaj, A. Varadwaj, H. M. Marques, K. Yamashita, Int. J. Mol. Sci. 2023, 24, 6659.
- [62] A. Kerckhoffs, K. E. Christensen, M. J. Langton, Chem. Sci. 2022, 13, 11551-11559.
- [63] P. Metrangolo, L. Canil, A. Abate, G. Terraneo, G. Cavallo, Angew. Chem. Int. Ed. 2022, 61, e202114793.
- [64] W. Zierkiewicz, R. Wysokiński, M. Michalczyk, S. Scheiner, ChemPhysChem 2020, 21, 870-877.
- [65] S. Scheiner, R. Wysokiński, M. Michalczyk, W. Zierkiewicz, J. Phys. Chem. A 2020, 124, 4998-5006.
- [66] A. Grabarz, M. Michalczyk, W. Zierkiewicz, S. Scheiner, Molecules 2021, 26, 2116.
- [67] A. Bauzá, A. Frontera, T. J. Mooibroek, Nat. Comm. 2017, 8, 14522.
- [68] A. Daolio, A. Pizzi, G. Terraneo, M. Ursini, A. Frontera, G. Resnati, Angew. Chem. Int. Ed. 2021, 60, 14385-14389.
- [69] Y. Zhao, D. G. Truhlar, Theor. Chem. Acc. 2008, 120, 215-241.
- [70] L. F. Molnar, X. He, B. Wang, K. M. Merz, J. Chem. Phys. 2009, 131, 065102.
- [71] M. A. Vincent, I. H. Hillier, Phys. Chem. Chem. Phys. 2011, 13, 4388-4392.
- [72] R. Podeszwa, K. Szalewicz, J. Chem. Phys. 2012, 136, 161102.
- [73] S. Karthikeyan, V. Ramanathan, B. K. Mishra, J. Phys. Chem. A 2013, 117, 6687-6694.
- [74] M. Majumder, B. K. Mishra, N. Sathyamurthy, Chem. Phys. 2013, 557, 59-65.
- [75] M. Walker, A. J. A. Harvey, A. Sen, C. E. H. Dessent, J. Phys. Chem. A 2013, 117, 12590-12600.
- [76] A. D. Boese, ChemPhysChem 2015, 16, 978-985.
- [77] B. S. D. R. Vamhindi, A. Karton, Chem. Phys. 2017, 493, 12-19.
- [78] M. J. Frisch, G. W. Trucks, H. B. Schlegel, G. E. Scuseria, M. A. Robb, J. R. Cheeseman, G. Scalmani, V. Barone, G. A. Petersson, H. Nakatsuji, X. Li, M. Caricato, A. V. Marenich, J. Bloino, B. G. Janesko, R. Gomperts, B. Mennucci, H. P. Hratchian, J. V. Ortiz, A. F. Izmaylov, J. L. Sonnenberg, D. Williams-Young, F. Ding, F. Lipparini, F. Egidi, J. Goings, B. Peng, A. Petrone, T. Henderson, D. Ranasinghe, V. G. Zakrzewski, J. Gao, N. Rega, G. Zheng, W. Liang, M. Hada, M. Ehara, K. Toyota, R. Fukuda, J. Hasegawa, M. Ishida, T. Nakajima, Y. Honda, O. Kitao, H. Nakai, T. Vreven, K. Throssell, J. A. Montgomery Jr. J. E. Peralta, F. Ogliaro, M. J. Bearpark, J. J. Heyd, E. N. Brothers, K. N. Kudin, V. N. Staroverov, T. A. Keith, R. Kobayashi, J. Normand, K. Raghavachari, A. P. Rendell, J. C. Burant, S. S. Iyengar, J. Tomasi, M. Cossi, J. M. Millam, M. Klene, C. Adamo, R. Cammi, J. W. Ochterski, R. L. Martin, K. Morokuma, O. Farkas, J. B. Foresman, D. J. Fox, Gaussian, Inc, Wallingford, CT 2016.
- [79] S. F. Boys, F. Bernardi, Mol. Phys. 1970, 19, 553-566.
- [80] T. Lu, F. Chen, J. Comput. Chem. 2012, 33, 580-592.
- [81] R. F. W. Bader, Atoms in Molecules, A Quantum Theory, Clarendon Press, Oxford 1990.
- [82] T. A. Keith, TK, AlMAll, Gristmill Software, Overland Park KS 2013.
- [83] K. Szalewicz, B. Jeziorski, in Molecular Interactions. From Van der Waals to Strongly Bound Complexes (Ed: S. Scheiner), Wiley, New York, 1997, pp. 3-43.

- [84] R. Moszynski, P. E. S. Wormer, B. Jeziorski, A. van der Avoird, J. Chem. Phys. 1995, 103, 8058-8074.
- [85] D. G. A. Smith, L. A. Burns, A. C. Simmonett, R. M. Parrish, M. C. Schieber, R. Galvelis, P. Kraus, H. Kruse, R. D. Remigio, A. Alenaizan, A. M. James, S. Lehtola, J. P. Misiewicz, M. Scheurer, R. A. Shaw, J. B. Schriber, Y. Xie, Z. L. Glick, D. A. Sirianni, J. S. O'Brien, J. M. Waldrop, A. Kumar, E. G. Hohenstein, B. P. Pritchard, B. R. Brooks, H. F. Schaeferlll, A. Y. Sokolov, K. Patkowski, A. E. DePrincelll, U. Bozkaya, R. A. King, F. A. Evangelista, J. M. Turney, T. D. Crawford, C. D. Sherrill, J. Chem. Phys. **2020**, 152, 184108.
- [86] R. Wysokiński, M. Michalczyk, W. Zierkiewicz, S. Scheiner, Phys. Chem. Chem. Phys. 2021, 23, 4818-4828.
- S. Banik, T. Baishya, R. M. Gomila, A. Frontera, M. Barcelo-Oliver, A. K. Verma, J. Das, M. K. Bhattacharyya, Inorganics 2024, 12, 111.
- [88] S. R. Kass, J. Am. Chem. Soc. 2005, 127, 13098–13099.
- [89] A. Shokri, M. Ramezani, A. Fattahi, S. R. Kass, J. Phys. Chem. A 2013, 117, 9252-9258.
- [90] I. Mata, E. Molins, I. Alkorta, E. Espinosa, J. Phys. Chem. A 2015, 119, 183-194.
- [91] G. Frenking, G. F. Caramori, Angew. Chem. Int. Ed. 2015, 54, 2596-2599.
- [92] D. Quinonero, I. Alkorta, J. Elguero, Phys. Chem. Chem. Phys. 2016, 18, 27939-27950.
- [93] G. Wang, Z. Chen, Z. Xu, J. Wang, Y. Yang, T. Cai, J. Shi, W. Zhu, J. Phys. Chem. B 2016, 120, 610-620.
- [94] S. M. Chalanchi, I. Alkorta, J. Elguero, D. Quiñonero, ChemPhysChem 2017, 18, 3462-3468.
- [95] C. Wang, Y. Fu, L. Zhang, D. Danovich, S. Shaik, Y. Mo, J. Comput. Chem. 2018, 39, 481-487.
- [96] F. Weinhold, Inorg. Chem. 2018, 57, 2035-2044.
- [97] R. Barbas, R. Prohens, A. Bauzá, A. Franconetti, A. Frontera, Chem. Commun. 2019, 55, 115-118.
- [98] Í. Iribarren, M. M. Montero-Campillo, I. Alkorta, J. Elguero, D. Quiñonero, Phys. Chem. Chem. Phys. 2019, 21, 5796-5802.
- [99] S. G. Dash, T. S. Thakur, Phys. Chem. Chem. Phys. 2019, 21, 20647-20660.
- [100] Z. Zhu, G. Wang, Z. Xu, Z. Chen, J. Wang, J. Shi, W. Zhu, Phys. Chem. Chem. Phys. 2019, 21, 15106-15119.
- [101] J. M. Holthoff, E. Engelage, R. Weiss, S. M. Huber, Angew. Chem. Int. Ed. 2020, 59, 11150-11157.
- [102] R. Wysokiński, W. Zierkiewicz, M. Michalczyk, S. Scheiner, ChemPhysChem 2020, 21, 1119-1125.
- [103] C. Loy, J. M. Holthoff, R. Weiss, S. M. Huber, S. V. Rosokha, Chem. Sci. **2021**, 12, 8246-8251.
- [104] J. M. Holthoff, R. Weiss, S. V. Rosokha, S. M. Huber, Chem. Eur. J. 2021, *27*, 16530-16542.
- [105] D. Fan, L. Chen, C. Wang, S. Yin, Y. Mo, J. Chem. Phys. 2021, 155, 234302.
- [106] A. Daolio, A. Pizzi, G. Terraneo, A. Frontera, G. Resnati, ChemPhysChem 2021. 22. 2281-2285.
- [107] R. Wysokiński, W. Zierkiewicz, M. Michalczyk, S. Scheiner, ChemPhysChem 2021, 22, 818-821.
- [108] L. Andreo, R. M. Gomila, E. Priola, A. Giordana, S. Pantaleone, E. Diana, G. Mahmoudi, A. Frontera, Cryst. Growth Des. 2022, 22, 6539-6544
- [109] J. Li, Q. Feng, C. Wang, Y. Mo, Phys. Chem. Chem. Phys. 2023, 25, 15371-15381.
- [110] M. Michalczyk, W. Zierkiewicz, R. Wysokiński, S. Scheiner, Phys. Chem. Chem. Phys. 2021, 23, 25097-25106. [111] W. Zierkiewicz, M. Michalczyk, T. Maris, R. Wysokiński, S. Scheiner,
- Chem. Commun. 2021, 57, 13305-13308. [112] M. Calabrese, A. Pizzi, R. Beccaria, A. Frontera, G. Resnati,
- ChemPhysChem 2023, 24, e202300298. [113] R. Beccaria, A. Dhaka, M. Calabrese, A. Pizzi, A. Frontera, G. Resnati,
- Chem. Eur. J. 2024, 30, e202303641.
- [114] C. Martín-Fernández, M. M. Montero-Campillo, I. Alkorta, J. Phys. Chem. Lett. 2024, 15, 4105-4110.
- [115] J. S. Murray, P. Politzer, ChemPhysChem 2021, 22, 1201-1207.
- [116] L. Chen, Q. Feng, C. Wang, S. Yin, Y. Mo, J. Phys. Chem. A 2021, 125, 10428-10438.
- [117] D. Quiñonero, I. Alkorta, J. Elguero, ChemPhysChem 2020, 21, 1597-1607.
- [118] R. Wysokiński, W. Zierkiewicz, M. Michalczyk, S. Scheiner, *Phys. Chem.* Chem. Phys. 2021, 23, 13853-13861.
- [119] N. Liu, Z. Han, Y. Lu, Z. Xu, W. Zhu, H. Liu, Chem. Phys. 2024, 576, 112113.

Europe

- [120] T. Clark, J. S. Murray, P. Politzer, Phys. Chem. Chem. Phys. 2018, 20,
- [121] M. Jabłoński, Chem. Phys. Lett. 2020, 759, 137946.
- [122] R. Taylor, CrystEngComm 2020, 22, 7145–7151.
- [123] S. Scheiner, J. Comput. Chem. **2022**, 43, 1814–1824.
- [124] P. L. A. Popelier, J. Mol. Model. 2022, 28, 276.
- [125] S. Scheiner, CrystEngComm 2023, 25, 5060-5071.

[126] G. Roos, J. S. Murray, Phys. Chem. Chem. Phys. 2024, 26, 7592–7601.

Manuscript received: June 12, 2024 Accepted manuscript online: July 8, 2024 Version of record online: August 22, 2024